AIAA JOURNAL
Vol. 34, No. 5, May 1996

Vibratory Characteristics of Pretwisted Cantilever Trapezoids of Unsymmetric Laminates

K. M. Liew* and C. W. Lim†
Nanyang Technological University, 2263 Singapore

Treated in this paper is a theoretical investigation on the vibratory characteristics of twisted unsymmetric laminates. An approach based on the global energy principle is developed to examine the effects of initial twist upon the vibration response of cantilevered unsymmetric laminates of a trapezoidal planform. It employs the Ritz extremum energy principle with a set of admissible *pb*-2 shape functions. These kinematically orientated *pb*-2 shape functions are composed of the product of 1) mathematically complete two-dimensional orthogonally generated polynomials and 2) a basic function to ensure satisfaction of the geometric boundary conditions. Numerical convergence of the eigenvalues is established by increasing the degree of polynomial of the shape functions. Results covering wide ranges of angles of twist and fiber orientation for 2-ply, 4-ply and 8-ply unsymmetric graphite/epoxy laminates are presented. Several findings with respect to these results are highlighted and conclusions are drawn. Finally, a set of vibration mode shapes illustrating the effects of aspect ratio, chord ratio, angles of twist, and fiber orientation is also included.

I. Introduction

VIBRATION studies on turbomachinery blades have long been a topic of intensive research especially in compressor, turbine, and impeller design. Similar models can also be used to simulate larger rotating helicopter blades, windmills, and marine propellers. Early researchers depended very much on the use of beam theory in these studies. Undoubtedly the most comprehensive study on pretwisted cantilever blading is attributed to Carnegie,[1,2] Houbolt and Brooks,[3] and Montoya,[4] in which the beam modeling was extensively developed. Such modeling could be inaccurate in cases where the blade aspect ratio is small (less than two) or higher vibration modes are required. On the other hand, the theoretical analysis of two-dimensional blade problems was only confined to simple rectangular blade and small angle of twist.[5]

The twisted plate theory with algebraic polynomials as the Ritz displacement function was employed by Bridle[6] to analyze the vibration of thick plates and shells. The torsional vibration of pretwisted cantilevered plates was solved by Gupta and Rao[7] who assumed pure rotation without axial warping. A collection of results for vibrations of pretwisted cantilever plates by various analytical and computational methods from various sources was also performed and reported by Leissa et al.,[8] Keilb et al.,[9] and MacBain et al.[10] in a joint university/industry/government research collaboration. It was shown that various methods resulted in a wide disagreement in vibration frequencies for the isotropic pretwisted plates. Some experimental and three-dimensional solutions were also provided in these references.

Although there are many reports on vibrations of pretwisted cantilever plates, very few dealing with composite pretwisted plates can be found. A pioneering work by Chamis[11] investigated the vibrations of composite fan blades. Comparison with measured data was also performed. A recent paper by Qatu and Leissa[12] considered the free flexural vibrations of laminated pretwisted cantilever plates of rectangular planform (when untwisted). They used two-dimensional simple polynomials as the admissible function to approximate the deflection. Although some interesting frequencies and mode shapes were published, these data are confined to 3-ply rectangular symmetric laminates. None are available, to the authors' knowledge, on the vibration analyses of unsymmetrically laminated pretwisted cantilever plate having trapezoidal planform (while untwisted). Thus, the primary purpose of the present paper is to investigate the vibratory characteristics of the cantilever pretwisted unsymmetric laminated trapezoidal plates.

The method of solution adopted in this study is a nondiscretization numerical algorithm based on the extremum energy principle, which incorporates the Ritz minimizing procedure with a set of orthogonally generated mathematically complete *pb*-2 shape functions.[13,14] This energy approach overestimates the stiffness of the structure and, thus, induces upper bound eigenvalues with respect to the exact solutions. Convergence of frequency parameters is necessary to ensure adequate terms in the in-plane and transverse deflection functions. In generating the orthogonal polynomials, satisfaction of all of the geometric boundary conditions is always ensured through 1) the kinematically oriented basic function in the shape functions and 2) the recurrence formula in the orthogonalization procedure. Therefore, this method is extremely versatile to account for various types of boundary conditions, although only the cantilever plate is considered here. The difficulties of mesh generation and continuity conditions for the discretization methods are avoided. Furthermore, it does not require much computation memory and execution time since no domain discretization is needed. To establish the accuracy and reliability, a convergence and comparison study with available data from the literature is carried out.

To demonstrate the applicability and versatility of this method, numerical examples including the 2-ply, 4-ply, and 8-ply graphite/epoxy laminates are solved. A set of first known data covering wide ranges of angles of twist and fiber orientation is presented. The effects of chord ratios and aspect ratios are also examined.

II. Mathematical Formulation

Figure 1 shows a thin, fiber reinforced plate of trapezoidal planform with an angle of twist ψ. The cantilever composite plate is composed of unsymmetrically laminated plies with respect to the midplane as illustrated in Fig. 2. It is champed at edge $x = 0$. The laminates have equal thicknesses with overall thickness h. The chord ratio is denoted by c_r and the angle of fiber orientation is β. The vibration frequencies and mode shapes of this laminated plate are to be determined. The deflections are decomposed into three orthogonal components u, v, and w parallel to the x, y, and z axes, respectively.

Received June 30, 1993; revision received March 20, 1995; accepted for publication March 31, 1995.

*Senior Lecturer, Division of Engineering Mechanics, School of Mechanical and Production Engineering.

†Research Assistant, Division of Engineering Mechanics, School of Mechanical and Production Engineering; currently Postdoctoral Fellow, Department of Civil Engineering, University of Queensland, 4072 Australia.

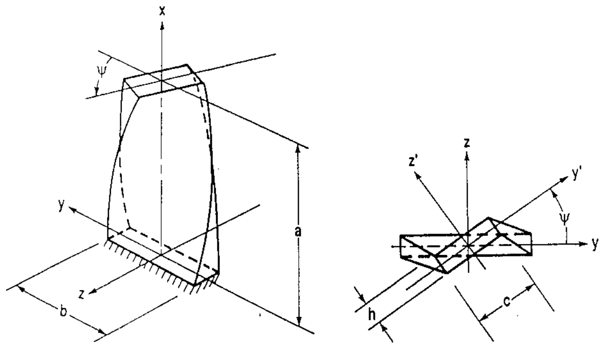

Fig. 1 Geometry of the pretwisted trapezoidal plate.

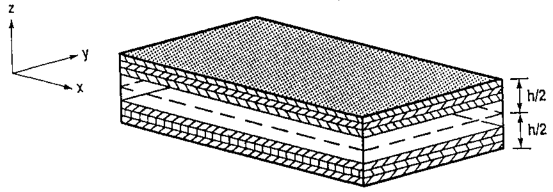

Fig. 2 Stacking sequence and fiber orientation of the unsymmetric laminates.

The strain energy $\mathcal{U}$ of the laminated plate can be expressed in terms of the volume integral as

$$\mathcal{U} = \frac{1}{2}\iiint_V (\sigma_x\epsilon_x + \sigma_y\epsilon_y + \sigma_{xy}\gamma_{xy})\,\mathrm{d}V \tag{1}$$

where the stress and strain of the kth laminate are related through transformed reduced stiffnesses $(\bar{Q}_{ij})_k$ in a matrix equation

$$\begin{Bmatrix} \sigma_x \\ \sigma_y \\ \sigma_{xy} \end{Bmatrix}_k = \begin{bmatrix} \bar{Q}_{11} & \bar{Q}_{12} & \bar{Q}_{16} \\ \bar{Q}_{12} & \bar{Q}_{22} & \bar{Q}_{26} \\ \bar{Q}_{16} & \bar{Q}_{26} & \bar{Q}_{66} \end{bmatrix}_k \begin{Bmatrix} \epsilon_x \\ \epsilon_y \\ \gamma_{xy} \end{Bmatrix}_k \tag{2}$$

Let c and s denote $\cos\beta_k$ and $\sin\beta_k$, respectively, then $(\bar{Q}_{ij})_k$ can be expressed in terms of the stiffness constants $(Q_{ij})_k$ and the fiber orientation angle β_k,

$$\bar{Q}_{11_k} = Q_{11_k}c^4 + 2\big(Q_{12_k} + 2Q_{66_k}\big)s^2c^2 + Q_{22_k}s^4 \tag{3a}$$

$$\bar{Q}_{12_k} = \big(Q_{11_k} + Q_{22_k} - 4Q_{66_k}\big)s^2c^2 + Q_{12_k}(s^4 + c^4) \tag{3b}$$

$$\bar{Q}_{22_k} = Q_{11_k}s^4 + 2\big(Q_{12_k} + 2Q_{66_k}\big)s^2c^2 + Q_{22_k}c^4 \tag{3c}$$

$$\begin{aligned}\bar{Q}_{16_k} &= \big(Q_{11_k} - Q_{12_k} - 2Q_{66_k}\big)sc^3 \\ &\quad + \big(Q_{12_k} - Q_{22_k} + 2Q_{66_k}\big)s^3c\end{aligned} \tag{3d}$$

$$\begin{aligned}\bar{Q}_{26_k} &= \big(Q_{11_k} - Q_{12_k} - 2Q_{66_k}\big)s^3c \\ &\quad + \big(Q_{12_k} - Q_{22_k} + 2Q_{66_k}\big)sc^3\end{aligned} \tag{3e}$$

$$\bar{Q}_{66_k} = \big(Q_{11_k} - 2Q_{12_k} + Q_{22_k} - 2Q_{66_k}\big)s^2c^2 + Q_{66_k}(s^4 + c^4) \tag{3f}$$

where

$$Q_{11_k} = \frac{E_{11_k}}{1 - \nu_{12_k}\nu_{21_k}} \tag{4a}$$

$$Q_{12_k} = \frac{\nu_{12_k}E_{22_k}}{1 - \nu_{12_k}\nu_{21_k}} \tag{4b}$$

$$Q_{22_k} = \frac{E_{22_k}}{1 - \nu_{12_k}\nu_{21_k}} \tag{4c}$$

$$Q_{66_k} = G_{12_k} \tag{4d}$$

$$\nu_{21_k}E_{11_k} = \nu_{12_k}E_{22_k} \tag{4e}$$

in which E_{11_k} and E_{22_k} are Young's moduli parallel and perpendicular to the fibers, respectively, and ν_{12_k} and ν_{21_k} are the corresponding Poisson ratios.

Substituting Eq. (2) into Eq. (1), the strain energy becomes

$$\begin{aligned}\mathcal{U} = \frac{1}{2}\iiint_V &\big(\bar{Q}_{11}\epsilon_x\epsilon_x + 2\bar{Q}_{12}\epsilon_x\epsilon_y + 2\bar{Q}_{16}\epsilon_x\gamma_{xy} \\ &+ \bar{Q}_{22}\epsilon_y\epsilon_y + 2\bar{Q}_{26}\epsilon_y\gamma_{xy} + \bar{Q}_{66}\gamma_{xy}\gamma_{xy}\big)\,\mathrm{d}V\end{aligned} \tag{5}$$

Using the following strain-displacement relationships[15]:

$$\begin{Bmatrix} \epsilon_x \\ \epsilon_y \\ \gamma_{xy} \end{Bmatrix} = \begin{Bmatrix} \dfrac{\partial u}{\partial x} \\ \dfrac{\partial v}{\partial y} \\ \dfrac{\partial u}{\partial y} + \dfrac{\partial v}{\partial x} + \dfrac{2w}{R_{xy}} \end{Bmatrix} - z \begin{Bmatrix} \dfrac{\partial^2 w}{\partial x^2} \\ \dfrac{\partial^2 w}{\partial y^2} \\ 2\dfrac{\partial^2 w}{\partial x \partial y} \end{Bmatrix} \tag{6}$$

the volume integral strain energy expression (5) can be reduced to surface integral over the domain of the plate planform as follows:

$$\begin{aligned}\mathcal{U} = \frac{1}{2}\iint_A \Bigg\{ & A_{11}\left(\frac{\partial u}{\partial x}\right)^2 + 2A_{12}\left(\frac{\partial u}{\partial x}\frac{\partial v}{\partial y}\right) + 2A_{16}\left(\frac{\partial u}{\partial x}\right) \\ & \times \left(\frac{\partial u}{\partial y} + \frac{\partial v}{\partial x} + \frac{2w}{R_{xy}}\right) + A_{22}\left(\frac{\partial u}{\partial y}\right)^2 \\ & + 2A_{26}\left(\frac{\partial v}{\partial y}\right)\left(\frac{\partial u}{\partial y} + \frac{\partial v}{\partial x} + \frac{2w}{R_{xy}}\right) + A_{66}\Bigg[\left(\frac{\partial u}{\partial y}\right)^2 \\ & + 2\left(\frac{\partial u}{\partial y}\frac{\partial v}{\partial x}\right) + \left(\frac{\partial v}{\partial x}\right)^2 + \left(\frac{4w}{R_{xy}}\right)\left(\frac{\partial u}{\partial y} + \frac{\partial v}{\partial x} + \frac{w}{R_{xy}}\right)\Bigg] \\ & - 2B_{11}\left(\frac{\partial u}{\partial x}\frac{\partial^2 w}{\partial x^2}\right) - 2B_{12}\left(\frac{\partial u}{\partial x}\frac{\partial^2 w}{\partial y^2} + \frac{\partial v}{\partial y}\frac{\partial^2 w}{\partial x^2}\right) \\ & - 2B_{22}\left(\frac{\partial v}{\partial y}\frac{\partial^2 w}{\partial y^2}\right) \\ & - 2B_{16}\left(\frac{\partial v}{\partial x}\frac{\partial^2 w}{\partial x^2} + \frac{\partial u}{\partial y}\frac{\partial^2 w}{\partial x^2} + 2\frac{\partial u}{\partial x}\frac{\partial^2 w}{\partial x \partial y} + \frac{2w}{R_{xy}}\frac{\partial^2 w}{\partial x^2}\right) \\ & - 2B_{26}\left(\frac{\partial v}{\partial x}\frac{\partial^2 w}{\partial y^2} + \frac{\partial u}{\partial y}\frac{\partial^2 w}{\partial y^2} + 2\frac{\partial v}{\partial y}\frac{\partial^2 w}{\partial x \partial y} + \frac{2w}{R_{xy}}\frac{\partial^2 w}{\partial y^2}\right) \\ & - 4B_{66}\left(\frac{\partial^2 w}{\partial x \partial y}\right)\left(\frac{\partial v}{\partial x} + \frac{\partial u}{\partial y} + \frac{2w}{R_{xy}}\right) \\ & + D_{11}\left(\frac{\partial^2 w}{\partial x^2}\right)^2 + 2D_{12}\left(\frac{\partial^2 w}{\partial x^2}\frac{\partial^2 w}{\partial y^2}\right) \\ & + 4D_{16}\left(\frac{\partial^2 w}{\partial x^2}\frac{\partial^2 w}{\partial x \partial y}\right) + D_{22}\left(\frac{\partial^2 w}{\partial y^2}\right)^2 \\ & + 4D_{26}\left(\frac{\partial^2 w}{\partial y^2}\frac{\partial^2 w}{\partial x \partial y}\right) + 4D_{66}\left(\frac{\partial^2 w}{\partial x \partial y}\right)^2 \Bigg\}\,\mathrm{d}A\end{aligned} \tag{7}$$

where A_{ij}, B_{ij}, and D_{ij} are the laminate stiffness coefficients given by

$$A_{ij} = \sum_{k=1}^{n}(\bar{Q}_{ij})_k(h_k - h_{k-1}) \qquad (i, j = 1, 2, 6) \tag{8a}$$

$$B_{ij} = \frac{1}{2}\sum_{k=1}^{n}(\bar{Q}_{ij})_k\big(h_k^2 - h_{k-1}^2\big) \qquad (i, j = 1, 2, 6) \tag{8b}$$

$$D_{ij} = \frac{1}{3}\sum_{k=1}^{n}(\bar{Q}_{ij})_k\left(h_k^3 - h_{k-1}^3\right) \qquad (i, j = 1, 2, 6) \tag{8c}$$

and ψ is related to the radius of twist R_{xy} by

$$\tan\psi = -(a/R_{xy}) \tag{9}$$

The kinetic energy for free vibration is given by

$$\mathcal{T} = \frac{\rho}{2}\iint_A\left[\left(\frac{\partial u}{\partial t}\right)^2 + \left(\frac{\partial v}{\partial t}\right)^2 + \left(\frac{\partial w}{\partial t}\right)^2\right]\mathrm{d}A \tag{10}$$

where ρ is the mass density per unit volume.

The deflection functions can be expressed in time periodic functions in the following forms:

$$u(x, y, t) = U(x, y)\sin\omega t \tag{11a}$$

$$v(x, y, t) = V(x, y)\sin\omega t \tag{11b}$$

$$w(x, y, t) = W(x, y)\sin\omega t \tag{11c}$$

where ω denotes the frequency of vibration.

The maximum strain energy $\mathcal{U}_{\max}$ and kinetic energy $\mathcal{T}_{\max}$ in a vibratory cycle can be derived by substituting Eqs. (11a–11c) into Eqs. (7) and (10).

The energy functional defined by the difference between the maximum strain and kinetic energies is

$$\Pi = \mathcal{U}_{\max} - \mathcal{T}_{\max} \tag{12}$$

which is to be minimized in accordance with the Ritz principle.

III. Method of Solution

Let a nondimensional coordinate system be

$$\xi = (x/a) \tag{13a}$$

$$\eta = (y/b) \tag{13b}$$

where a and b are the span and width of the plate planform as shown in Fig. 1. The in-plane and transverse deflection amplitude functions, $U(\xi, \eta)$, $V(\xi, \eta)$, and $W(\xi, \eta)$, can be approximated by a series of orthogonally generated two-dimensional polynomials of the forms

$$U(\xi, \eta) = \sum_{i=1}^{m} C_{ui}\phi_{ui}(\xi, \eta) \tag{14a}$$

$$V(\xi, \eta) = \sum_{i=1}^{m} C_{vi}\phi_{vi}(\xi, \eta) \tag{14b}$$

$$W(\xi, \eta) = \sum_{i=1}^{m} C_{wi}\phi_{wi}(\xi, \eta) \tag{14c}$$

where C_{ui}, C_{vi}, and C_{wi} are the unknown coefficients and ϕ_{ui}, ϕ_{vi}, and ϕ_{wi} are the corresponding pb-2 shape functions. The later are sets of orthogonally generated two-dimensional polynomials to be discussed in due course.

By minimizing the energy functional in Eq. (12) with respect to each of the coefficients,

$$\frac{\partial\Pi}{\partial C_{\alpha i}} = 0; \qquad \alpha = u, v \text{ and } w \tag{15}$$

the following governing eigenvalue equation can be obtained:

$$(12\boldsymbol{K} - \lambda^2\boldsymbol{M})\{\boldsymbol{C}\} = \{\boldsymbol{0}\} \tag{16}$$

where $\boldsymbol{K}$ is the stiffness matrix and $\boldsymbol{M}$ is the mass matrix expressed as follows:

$$\boldsymbol{K} = \begin{bmatrix} [K_{uu}] & [K_{uv}] & [K_{uw}] \\ & [K_{vv}] & [K_{vw}] \\ \text{sym} & & [K_{ww}] \end{bmatrix} \tag{17a}$$

$$\boldsymbol{M} = \begin{bmatrix} [M_{uu}] & [0] & [0] \\ & [M_{vv}] & [0] \\ \text{sym} & & [M_{ww}] \end{bmatrix} \tag{17b}$$

and the vector of unknown coefficients is

$$\{\boldsymbol{C}\} = \begin{Bmatrix} \{C_{uj}\} \\ \{C_{vj}\} \\ \{C_{wj}\} \end{Bmatrix} \tag{17c}$$

The elements in the stiffness and mass matrices are

$$K_{uuij} = \frac{b^2A_{11}}{D_0}\mathcal{I}_{uiuj}^{1010} + \frac{abA_{16}}{D_0} \times\left(\mathcal{I}_{uiuj}^{0110} + \mathcal{I}_{uiuj}^{1001}\right) + \frac{a^2A_{66}}{D_0}\mathcal{I}_{uiuj}^{0101} \tag{18a}$$

$$K_{uvij} = \frac{abA_{12}}{D_0}\mathcal{I}_{uivj}^{1001} + \frac{b^2A_{16}}{D_0}\mathcal{I}_{uivj}^{1010} + \frac{a^2A_{26}}{D_0}\mathcal{I}_{uivj}^{0101} + \frac{abA_{66}}{D_0}\mathcal{I}_{uivj}^{0110} \tag{18b}$$

$$K_{uwij} = \frac{2ab^2A_{16}}{R_{xy}D_0}\mathcal{I}_{uiwj}^{1000} + \frac{2a^2bA_{66}}{R_{xy}D_0}\mathcal{I}_{uiwj}^{0100} - \frac{b^2B_{11}}{aD_0}\mathcal{I}_{uiwj}^{1020} - \frac{aB_{12}}{D_0}\mathcal{I}_{uiwj}^{1002} - \frac{bB_{16}}{D_0}\left(\mathcal{I}_{uiwj}^{0120} + 2\mathcal{I}_{uiwj}^{1011}\right) - \frac{a^2B_{26}}{bD_0}\mathcal{I}_{uiwj}^{0102} - \frac{2aB_{66}}{D_0}\mathcal{I}_{uiwj}^{0111} \tag{18c}$$

$$K_{vvij} = \frac{a^2A_{22}}{D_0}\mathcal{I}_{vivj}^{0101} + \frac{abA_{26}}{D_0} \times\left(\mathcal{I}_{vivj}^{0110} + \mathcal{I}_{vivj}^{1001}\right) + \frac{b^2A_{66}}{D_0}\mathcal{I}_{vivj}^{1010} \tag{18d}$$

$$K_{vwij} = \frac{2a^2bA_{26}}{R_{xy}D_0}\mathcal{I}_{viwj}^{0100} + \frac{2ab^2A_{66}}{R_{xy}D_0}\mathcal{I}_{viwj}^{1000} - \frac{bB_{12}}{D_0}\mathcal{I}_{viwj}^{0120} - \frac{b^2B_{16}}{aD_0}\mathcal{I}_{viwj}^{1020} - \frac{a^2B_{22}}{bD_0}\mathcal{I}_{viwj}^{0102} - \frac{aB_{26}}{D_0}\left(\mathcal{I}_{viwj}^{1002} + 2\mathcal{I}_{viwj}^{0111}\right) - \frac{2bB_{66}}{D_0}\mathcal{I}_{viwj}^{1011} \tag{18e}$$

$$K_{wwij} = \frac{4a^2b^2A_{66}}{R_{xy}^2D_0}\mathcal{I}_{wiwj}^{0000} - \frac{2b^2B_{16}}{R_{xy}D_0}\left(\mathcal{I}_{wiwj}^{2000} + \mathcal{I}_{wiwj}^{0020}\right) - \frac{2a^2B_{26}}{R_{xy}D_0}\left(\mathcal{I}_{wiwj}^{0200} + \mathcal{I}_{wiwj}^{0002}\right) - \frac{4abB_{66}}{R_{xy}D_0}\left(\mathcal{I}_{wiwj}^{1100} + \mathcal{I}_{wiwj}^{0011}\right) + \frac{b^2D_{11}}{a^2D_0}\mathcal{I}_{wiwj}^{2020} + \frac{D_{12}}{D_0}\left(\mathcal{I}_{wiwj}^{0220} + \mathcal{I}_{wiwj}^{2002}\right) + \frac{2bD_{16}}{aD_0} \times\left(\mathcal{I}_{wiwj}^{1120} + \mathcal{I}_{wiwj}^{2011}\right) + \frac{a^2D_{22}}{b^2D_0}\mathcal{I}_{wiwj}^{0202} + \frac{2aD_{26}}{bD_0}\left(\mathcal{I}_{wiwj}^{1102} + \mathcal{I}_{wiwj}^{0211}\right) + \frac{4D_{66}}{D_0}\mathcal{I}_{wiwj}^{1111} \tag{18f}$$

$$M_{uuij} = \mathcal{I}_{uiuj}^{0000} \tag{18g}$$

$$M_{vvij} = \mathcal{I}_{vivj}^{0000} \tag{18h}$$

$$M_{wwij} = \mathcal{I}_{wiwj}^{0000} \tag{18i}$$

$$\lambda = \omega ab\sqrt{\frac{\rho h}{D_0}} \tag{18j}$$

where

$$\mathcal{I}_{uiuj}^{defg} = \int\int_A \frac{\partial^{d+e}\phi_{ui}(\xi,\eta)}{\partial\xi^d\partial\eta^e}\frac{\partial^{f+g}\phi_{uj}(\xi,\eta)}{\partial\xi^f\partial\eta^g}\,\mathrm{d}\xi\,\mathrm{d}\eta \tag{19a}$$

$$\mathcal{I}_{uivj}^{defg} = \int\int_A \frac{\partial^{d+e}\phi_{ui}(\xi,\eta)}{\partial\xi^d\partial\eta^e}\frac{\partial^{f+g}\phi_{vj}(\xi,\eta)}{\partial\xi^f\partial\eta^g}\,\mathrm{d}\xi\,\mathrm{d}\eta \tag{19b}$$

$$\mathcal{I}_{uiwj}^{defg} = \int\int_A \frac{\partial^{d+e}\phi_{ui}(\xi,\eta)}{\partial\xi^d\partial\eta^e}\frac{\partial^{f+g}\phi_{wj}(\xi,\eta)}{\partial\xi^f\partial\eta^g}\,\mathrm{d}\xi\,\mathrm{d}\eta \tag{19c}$$

$$\mathcal{I}_{vivj}^{defg} = \int\int_A \frac{\partial^{d+e}\phi_{vi}(\xi,\eta)}{\partial\xi^d\partial\eta^e}\frac{\partial^{f+g}\phi_{vj}(\xi,\eta)}{\partial\xi^f\partial\eta^g}\,\mathrm{d}\xi\,\mathrm{d}\eta \tag{19d}$$

$$\mathcal{I}_{viwj}^{defg} = \int\int_A \frac{\partial^{d+e}\phi_{vi}(\xi,\eta)}{\partial\xi^d\partial\eta^e}\frac{\partial^{f+g}\phi_{wj}(\xi,\eta)}{\partial\xi^f\partial\eta^g}\,\mathrm{d}\xi\,\mathrm{d}\eta \tag{19e}$$

$$\mathcal{I}_{wiwj}^{defg} = \int\int_A \frac{\partial^{d+e}\phi_{wi}(\xi,\eta)}{\partial\xi^d\partial\eta^e}\frac{\partial^{f+g}\phi_{wj}(\xi,\eta)}{\partial\xi^f\partial\eta^g}\,\mathrm{d}\xi\,\mathrm{d}\eta \tag{19f}$$

and $i, j = 1, 2, \ldots, m$. The double integrations are symmetric in nature, that is, $\mathcal{I}_{\alpha i\beta j}^{defg} = \mathcal{I}_{\beta j\alpha i}^{fgde}$. The reference plate flexural rigidity is $D_0 = Q_{11}h^3/12 = E_{11}h^3/12(1-\nu_{12}\nu_{21})$ and λ is the nondimensional frequency parameter that appears as the eigenvalue in Eq. (16).

As stated in Eqs. (14a–14c), the pb-2 shape functions $\phi_{\alpha i}$, ($\alpha = u$, v, and w) are individually a set of admissible functions consisting the product of terms (indicated by i) of a mathematically complete two-dimensional orthogonally generated polynomials (p-2) and a basic function ($\phi_{\alpha b}$), i.e.,

$$\phi_{\alpha i}(\xi,\eta) = f_i(\xi,\eta)\phi_{\alpha b} - \sum_{j=1}^{i-1}\Xi_{\alpha ij}\phi_{\alpha j} \tag{20}$$

where

$$\Xi_{\alpha ij} = \left[\int\int_A f_i(\xi,\eta)\phi_{\alpha b}\phi_{\alpha j}\,\mathrm{d}\xi\,\mathrm{d}\eta \Big/ \int\int_A \phi_{\alpha j}^2\,\mathrm{d}\xi\,\mathrm{d}\eta\right]; \quad \alpha = u, v, \text{ and } w \tag{21a}$$

The summation $\sum_{i=1}^{m} f_i(\xi,\eta)$ forms a complete set of p-2 functions, and $\phi_{\alpha b}(\alpha = u, v$ and $w)$ are the basic functions defined by the products of the equations of the continuous piecewise boundary geometries of the plate planform, each of which is raised to an appropriate power.

Using the recurrence procedure, for instance, the pb-2 shape functions for the first six terms can be generated as

$$\phi_{\alpha 1}(x,y) = \phi_{\alpha b}(x,y) \tag{22a}$$

$$\phi_{\alpha 2}(x,y) = x\phi_{\alpha 1}(x,y) - \Xi_{\alpha 21}\phi_{\alpha 1}(x,y) \tag{22b}$$

$$\phi_{\alpha 3}(x,y) = y\phi_{\alpha 1}(x,y) - \Xi_{\alpha 31}\phi_{\alpha 1}(x,y) - \Xi_{\alpha 32}\phi_{\alpha 2}(x,y) \tag{22c}$$

$$\phi_{\alpha 4}(x,y) = x^2\phi_{\alpha 1}(x,y) - \Xi_{\alpha 41}\phi_{\alpha 1}(x,y) - \Xi_{\alpha 42}\phi_{\alpha 2}(x,y) - \Xi_{\alpha 43}\phi_{\alpha 3}(x,y) \tag{22d}$$

$$\phi_{\alpha 5}(x,y) = xy\phi_{\alpha 1}(x,y) - \Xi_{\alpha 51}\phi_{\alpha 1}(x,y) - \Xi_{\alpha 52}\phi_{\alpha 2}(x,y) - \Xi_{\alpha 53}\phi_{\alpha 3}(x,y) - \Xi_{\alpha 54}\phi_{\alpha 4}(x,y) \tag{22e}$$

$$\phi_{\alpha 6}(x,y) = y^2\phi_{\alpha 1}(x,y) - \Xi_{\alpha 61}\phi_{\alpha 1}(x,y) - \Xi_{\alpha 62}\phi_{\alpha 2}(x,y) - \Xi_{\alpha 63}\phi_{\alpha 3}(x,y) - \Xi_{\alpha 64}\phi_{\alpha 4}(x,y) - \Xi_{\alpha 65}\phi_{\alpha 5}(x,y) \tag{22f}$$

In the present approach, the basic functions for different boundary conditions are given by

$$\phi_{ub}(\xi,\eta) = \prod_{i=1}^{n_e}[\Gamma_i(\xi,\eta)]^{\gamma_{ui}}$$

$$\gamma_{ui} = \begin{cases} 0 & \text{free} \\ 1 & u\text{-deflection constrained} \end{cases} \tag{23a}$$

$$\phi_{vb}(\xi,\eta) = \prod_{i=1}^{n_e}[\Gamma_i(\xi,\eta)]^{\gamma_{vi}}$$

$$\gamma_{ui} = \begin{cases} 0 & \text{free} \\ 1 & v\text{-deflection constrained} \end{cases} \tag{23b}$$

$$\phi_{wb}(\xi,\eta) = \prod_{i=1}^{n_e}[\Gamma_i(\xi,\eta)]^{\gamma_{wi}}$$

$$\gamma_{wi} = \begin{cases} 0 & \text{free} \\ 1 & \text{simply supported} \\ 2 & \text{clamped} \end{cases} \tag{23c}$$

where n_e is the number of supporting edges and Γ_i is the boundary expression of the ith supporting edge. In the present study, $i = 1$ refers to the edge at $x = 0$, and $i = 2, 3, 4$ correspond to the subsequent edges going anticlockwise. For the arbitrarily supported trapezoidal plate under consideration (see Fig. 1), the basic functions in terms of nondimensional coordinates are

$$\phi_{\alpha b}(\xi,\eta) = \xi^{\gamma_{\alpha 1}}(\xi-1)^{\gamma_{\alpha 3}}\left[\eta + \frac{1}{2}\left(\frac{c}{b}-1\right)\xi + \frac{1}{2}\right]^{\gamma_{\alpha 2}} \times \left[\eta + \frac{1}{2}\left(1-\frac{c}{b}\right)\xi - \frac{1}{2}\right]^{\gamma_{\alpha 4}} \tag{24}$$

where $\alpha = u$, v, and w and a/b is the aspect ratio, c/b (or c_r) is the chord ratio, $\gamma_{\alpha i}(\alpha = u, v$ and w; $i = 1, 2, 3, 4)$ are the powers of assigned values with either 0, 1, or 2 depending whether the normal, tangential, or the transverse deflection is constrained.

The mathematically complete two-dimensional polynomial $\sum_{i=1}^{m} f_i(\xi,\eta)$ on the other hand, can be expressed as

$$\sum_{i=1}^{m} f_i(\xi,\eta) = \sum_{q=0}^{p}\sum_{i=0}^{q}\xi^{q-i}\eta^i \tag{25}$$

with m and p related by

$$m = [(p+1)(p+2)/2] \tag{26}$$

where p is the degree of the complete set of two-dimensional polynomials to be employed.

IV. Numerical Studies

To demonstrate the applicability and numerical accuracy of the proposed method, a convergence study is carried out and the results are compared with available data. The material used in the present study is graphite/epoxy (G/E) where $E_{11} = 138$ GPa, $E_{22} = 8.96$ GPa, $G_{12} = 7.1$ GPa, and $\nu_{12} = 0.3$. The effects of angle of twist, fiber orientation and stacking sequences on the nondimensional vibration frequencies $\lambda = \omega ab\sqrt{(\rho h/D_o)}$ are investigated. For plates with varying aspects ratio (a/b), we may assume that the product ab

Table 1 Convergence of $\lambda = \omega ab\sqrt{(\rho h/D_0)}$ for the 8-ply pretwisted graphite/epoxy plate with $a/b = 1.0$, $b/h = 100.0$, and stacking sequence $(\beta, -\beta, \beta, -\beta, \beta, -\beta, \beta, -\beta)$

c_r	ψ, deg	β, deg	p: u	v	w	Mode sequence number: 1	2	3	4	5	6	7	8
			10	10	10	2.4902	14.925	30.663	34.185	40.680	45.105	58.862	64.589
			10	10	11	2.4888	14.921	30.659	34.185	40.678	45.092	58.856	64.562
			10	10	12	2.4878	14.917	30.658	34.184	40.677	45.085	58.825	64.550
			10	10	13	2.4871	14.914	30.658	34.184	40.676	45.076	58.825	64.548
			10	10	14	2.4865	14.912	30.657	34.184	40.676	45.070	58.824	64.547
			10	10	15	2.4862	14.910	30.656	34.183	40.676	45.066	58.823	64.547
			10	10	16	2.4859	14.908	30.655	34.183	40.676	45.062	58.823	64.547
			10	10	17	2.4857	14.907	30.655	34.183	40.676	45.059	58.823	64.547
1.0	30	30	10	10	18	2.4856	14.906	30.654	34.182	40.676	45.057	58.822	64.547
			10	11	18	2.4856	14.906	30.649	34.179	40.674	45.056	58.814	64.526
			10	12	18	2.4855	14.906	30.646	34.174	40.673	45.055	58.813	64.509
			10	13	18	2.4855	14.906	30.644	34.171	40.672	45.055	58.813	64.502
			10	14	18	2.4855	14.906	30.643	34.170	40.672	45.055	58.812	64.495
			11	14	18	2.4854	14.906	30.641	34.168	40.671	45.050	58.807	64.483
			12	14	18	2.4854	14.906	30.640	34.165	40.670	45.050	58.807	64.477
			13	14	18	2.4854	14.906	30.639	34.164	40.670	45.049	58.806	64.474
			14	14	18	2.4854	14.906	30.638	34.164	40.670	45.049	58.806	64.469
			10	10	10	1.3273	6.9537	20.804	42.160	49.777	59.305	72.038	83.339
			10	10	11	1.3269	6.9515	20.799	42.142	49.771	59.286	71.953	83.324
			10	10	12	1.3267	6.9501	20.795	42.135	49.766	59.278	71.916	83.306
			10	10	13	1.3266	6.9491	20.793	42.131	49.766	59.278	71.888	83.304
			10	10	14	1.3265	6.9485	20.791	42.127	49.765	59.276	71.883	83.300
			10	10	15	1.3264	6.9480	20.789	42.124	49.765	59.276	71.878	83.298
			10	10	16	1.3264	6.9477	20.788	42.122	49.765	59.276	71.875	83.298
			10	10	17	1.3264	6.9475	20.788	42.121	49.765	59.276	71.872	83.297
0.5	45	60	10	10	18	1.3264	6.9474	20.787	42.120	49.765	59.276	71.870	83.297
			10	11	18	1.3263	6.9473	20.787	42.119	49.764	59.271	71.802	83.279
			10	12	18	1.3263	6.9473	20.787	42.119	49.763	59.268	71.799	83.276
			10	13	18	1.3263	6.9473	20.787	42.118	49.763	59.267	71.797	83.272
			10	14	18	1.3263	6.9473	20.787	42.118	49.762	59.267	71.797	83.270
			11	14	18	1.3263	6.9472	20.786	42.107	49.760	59.266	71.781	83.251
			12	14	18	1.3263	6.9472	20.786	42.106	49.758	59.265	71.762	83.246
			13	14	18	1.3263	6.9472	20.786	42.105	49.757	59.264	71.757	83.244
			14	14	18	1.3263	6.9472	20.786	42.105	49.757	59.264	71.755	83.242

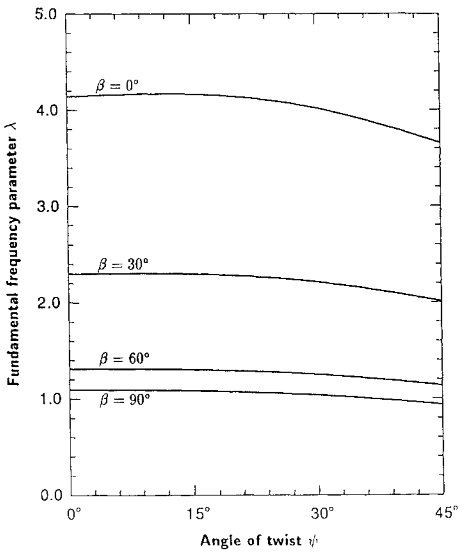

Fig. 3 Effects of angle of twist on the nondimensional fundamental frequency $\lambda = \omega ab\sqrt{(\rho h/D_0)}$ for the 2-ply graphite/epoxy plate with $a/b = 1.0$, $b/h = 100.0$, $c_r = 0.5$, and stacking sequence $(\beta, -\beta)$.

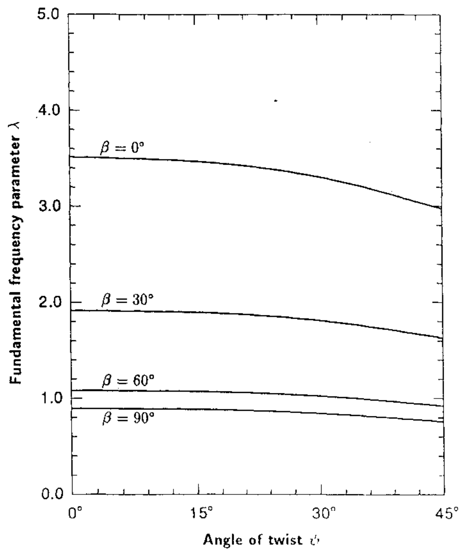

Fig. 4 Effects of angle of twist on the nondimensional fundamental frequency $\lambda = \omega ab\sqrt{(\rho h/D_0)}$ for the 2-ply graphite/epoxy plate with $a/b = 1.0$, $b/h = 100.0$, $c_r = 1.0$, and stacking sequence $(\beta, -\beta)$.

is invariant. Thus, the physical frequency of vibration ω is directly proportional to λ.

Table 1 shows the convergence of eigenvalues for the 8-ply pretwisted unsymmetrically laminated square plate with stacking sequence $(\beta, -\beta, \beta, -\beta, \beta, -\beta, \beta, -\beta)$. The degrees of polynomial for u, v, and w are increased to achieve the desired level of convergence. The convergence of eigenvalues follows a direct downward trend because the Ritz minimizing procedure always overestimates the stiffness of the plate which results in higher frequency parameters with respect to exact solutions. However, upper-bound frequency parameters can be found by increasing the degrees of polynomial of the *pb*-2 shape functions. From Table 1, it is obvious that the respectively degrees of polynomial may not be the same but, in general degrees 14, 14, and 18 for u, v, and w (a determinant size of 430 × 430) are sufficient to reach an acceptable convergence up to four significant figures.

Table 2 Comparison of frequency parameter $\omega a^2\sqrt{(\rho/E_{11}h^3)}$ for the pretwisted 3-ply graphite/epoxy plate with a/b = 1.0, c_r = 1.0, b/h = 100.0, ψ = 45 deg, and stacking sequence (β, $-\beta$, β)

β, deg	Reference	Mode sequence number 1	2	3	4	5	6	7	8	9	10
0	Qatu and Leissa[12]	0.8608	5.1012	12.764	14.449	15.861	16.347	21.273	25.315	26.535	27.149
	Present	0.86071	5.0989	12.634	14.257	15.614	16.303	21.140	24.166	25.673	26.470
15	Qatu and Leissa[12]	0.8045	4.7551	12.950	14.121	15.335	16.204	22.142	27.126	27.803	28.343
	Present	0.80399	4.7465	12.725	13.992	15.086	15.917	21.920	24.690	26.968	27.531
30	Qatu and Leissa[12]	0.6549	3.8350	11.708	11.967	14.012	15.750	22.133	26.077	27.522	28.092
	Present	0.65311	3.8219	11.599	11.827	13.849	15.328	21.672	24.052	25.019	25.690
45	Qatu and Leissa[12]	0.4698	2.7296	8.6002	10.393	12.140	16.325	21.310	22.814	24.553	26.219
	Present	0.46664	2.7166	8.4729	10.283	11.995	15.465	17.887	20.955	22.440	24.308
60	Qatu and Leissa[12]	0.3135	1.8384	5.9160	9.4600	13.645	17.099	18.990	19.603	22.953	25.397
	Present	0.31196	1.8289	5.8045	9.3802	10.562	11.949	17.060	18.721	20.105	22.558
75	Qatu and Leissa[12]	0.2352	1.3984	4.5249	9.1080	9.6967	14.908	18.416	18.704	20.719	23.661
	Present	0.23485	1.3941	4.4454	9.0412	9.1208	9.6683	15.314	18.236	18.489	20.443
90	Qatu and Leissa[12]	0.2192	1.3058	4.2192	9.1152	9.2419	12.747	17.889	18.888	19.675	20.771
	Present	0.21919	1.3031	4.1607	8.4707	9.0989	9.2623	14.285	17.738	18.805	19.624

Table 3 Frequency parameters $\lambda = \omega ab\sqrt{(\rho h/D_0)}$ for the cantilever pretwisted 2-ply graphite/epoxy plate with b/h = 100.0 and stacking sequence (β, $-\beta$)

a/b	ψ, deg	β, deg	c_r	Mode sequence number 1	2	3	4	5	6	7	8
		30	0.5	2.2978	7.5985	12.387	21.915	21.932	32.910	40.983	43.481
	0		1.0	1.9143	4.4762	10.294	12.176	16.496	22.297	26.567	33.588
		60	0.5	1.3123	6.7322	7.1304	18.143	19.230	28.694	33.214	37.387
			1.0	1.0818	3.9421	6.7189	13.047	14.198	19.122	26.084	26.150
		30	0.5	2.2959	12.316	25.361	30.687	33.906	38.726	50.939	53.675
	15		1.0	1.8925	11.650	16.948	19.270	24.809	33.290	34.317	40.415
		60	0.5	1.2995	7.0076	15.455	19.105	31.234	32.313	37.275	45.760
1.0			1.0	1.0684	6.5833	11.947	16.334	19.086	27.149	35.124	36.471
		30	0.5	2.2119	11.707	32.881	45.294	49.206	61.553	64.400	68.715
	30		1.0	1.8071	10.831	27.574	31.025	33.117	35.901	51.053	60.693
		60	0.5	1.2495	6.6395	18.715	29.678	36.764	40.057	51.350	60.700
			1.0	1.0207	6.1473	18.165	21.871	22.414	36.556	42.036	45.438
		30	0.5	2.0113	10.587	31.590	63.043	66.569	72.013	83.777	95.596
	45		1.0	1.6287	9.5815	30.611	39.931	43.547	50.045	62.489	71.320
		60	0.5	1.1366	6.0138	17.956	36.030	48.135	51.288	60.570	69.717
			1.0	0.92020	5.4491	17.397	30.766	31.097	35.667	56.224	60.111
		30	0.5	1.1541	6.2724	6.6288	16.924	17.639	30.795	31.812	33.010
	0		1.0	0.94985	3.8774	5.9065	12.647	15.338	17.071	24.640	26.689
		60	0.5	0.65369	3.5565	6.1803	9.5942	15.769	18.669	26.879	30.812
			1.0	0.53561	3.3431	3.6113	9.4072	11.232	18.490	20.035	25.404
		30	0.5	1.1442	6.1637	15.750	16.825	32.673	32.875	34.636	48.397
	15		1.0	0.93904	5.7830	12.575	16.247	18.072	27.990	32.625	36.235
		60	0.5	0.64596	3.4908	9.4899	9.5255	18.587	21.506	30.719	34.706
2.0			1.0	0.52872	3.2652	6.9296	9.3238	18.411	20.240	25.471	30.778
		30	0.5	1.1005	5.8382	16.479	30.482	32.408	42.471	53.860	56.120
	30		1.0	0.89754	5.3981	16.052	23.578	23.866	32.166	42.381	47.891
		60	0.5	0.61954	3.2977	9.3181	16.257	18.360	30.474	34.038	45.554
			1.0	0.50520	3.0428	9.0785	13.049	18.180	26.068	30.661	35.717
		30	0.5	1.0011	5.2875	15.800	31.707	49.859	52.192	55.369	77.089
	45		1.0	0.80943	4.7854	15.308	31.320	33.143	34.176	52.890	55.494
		60	0.5	0.56342	2.9807	8.9291	17.948	26.238	30.042	45.160	52.377
			1.0	0.45601	2.7006	8.6513	17.753	21.450	27.809	30.598	44.880

Having established the numerical convergence, a comparison study with available frequency data[12] is carried out to check the reliability of the present approach. The comparison is presented in Table 2 using a 3-ply G/E pretwisted plate with square planform (a/b = 1.0 and c_r = 1.0), thickness ratio b/h = 100, and laminate stacking sequence (β, $-\beta$, β). The frequency parameter in this case is $\omega a^2\sqrt{(\rho/E_{11}h^3)}$. Excellent agreement between the results is achieved. It is also noticed that the present result is consistently lower than the results of Qatu and Leissa,[12] who also employed the Ritz method but with different shape functions. Keeping in mind that the Ritz method overestimates the stiffness and vibration frequencies and yields upper bound eigenvalues, the present results are more accurate because a total of 430 terms have been used with respect to 144 terms used by Qatu and Leissa.[12]

The present method is subsequently employed to investigate the vibration behavior of cantilever trapezoidal graphite/epoxy plate with unsymmetric staking sequence. In this study, the thickness

Table 4 Frequency parameters $\lambda = \omega ab\sqrt{(\rho h/D_0)}$ for the cantilever pretwisted 4-ply graphite/epoxy plate with b/h = 100.0 and stacking sequence $(-\beta, \beta, -\beta, \beta)$

a/b	ψ, deg	β, deg	c_r	Mode sequence number 1	2	3	4	5	6	7	8
		30	0.5	2.9867	10.124	15.834	27.584	28.896	42.994	53.826	56.253
	0		1.0	2.5041	6.0253	12.757	16.136	21.526	27.148	35.735	43.493
		60	0.5	1.4706	7.8924	8.9616	21.568	23.735	37.984	42.499	42.672
			1.0	1.2180	5.2670	7.4354	17.029	18.176	22.285	32.636	35.212
		30	0.5	2.9838	15.959	27.772	35.432	42.287	44.111	62.799	63.206
	15		1.0	2.4745	15.132	18.524	21.196	28.555	37.960	43.508	47.389
		60	0.5	1.4603	7.7882	16.631	21.465	35.947	40.079	42.984	55.017
1.0			1.0	1.2058	7.3406	12.879	19.312	22.585	31.234	41.401	43.603
		30	0.5	2.8835	15.360	42.724	50.690	54.394	64.955	78.472	83.490
	30		1.0	2.3627	14.271	29.925	33.364	40.495	43.061	58.756	63.794
		60	0.5	1.4121	7.4384	21.087	30.557	41.655	47.617	58.940	69.065
			1.0	1.1566	6.9410	20.408	24.253	25.732	42.017	47.772	53.090
		30	0.5	2.6273	13.981	41.560	74.276	78.044	83.866	91.732	104.45
	45		1.0	2.1298	12.688	39.705	42.608	47.203	55.807	78.978	83.167
		60	0.5	1.2922	6.8017	20.331	41.136	49.364	57.524	69.873	82.593
			1.0	1.0467	6.2045	19.806	33.929	35.826	41.060	59.001	69.418
		30	0.5	1.4750	7.9151	8.9699	21.630	23.765	37.944	42.572	42.781
	0		1.0	1.2216	5.2720	7.4566	17.052	18.158	22.332	32.704	35.208
		60	0.5	0.71503	3.8626	8.3671	10.533	20.735	21.180	34.514	35.680
			1.0	0.58882	3.6459	4.8993	10.402	15.092	20.665	26.457	32.417
		30	0.5	1.4635	7.8120	17.013	21.516	35.933	40.311	43.139	53.845
	15		1.0	1.2086	7.3623	13.042	19.404	22.684	30.926	41.587	43.117
		60	0.5	0.70753	3.7961	10.467	11.119	20.670	26.064	34.441	42.706
2.0			1.0	0.58211	3.5685	7.7295	10.328	20.619	23.135	32.372	36.022
		30	0.5	1.4148	7.4626	21.138	31.551	41.805	48.388	58.997	69.468
			1.0	1.1592	6.9624	20.475	24.508	26.163	42.112	48.275	53.584
		60	0.5	0.68136	3.5942	10.258	17.395	20.457	34.214	37.843	51.450
			1.0	0.55858	3.3398	10.093	13.629	20.443	32.310	36.228	39.580
		30	0.5	1.2947	6.8232	20.386	41.256	51.478	59.185	70.210	82.890
	45		1.0	1.0490	6.2235	19.860	34.826	36.059	41.174	61.975	69.659
		60	0.5	0.62422	3.2609	9.8639	20.056	27.099	33.811	51.107	56.426
			1.0	0.50759	2.9822	9.6657	20.068	22.194	32.601	36.900	51.075

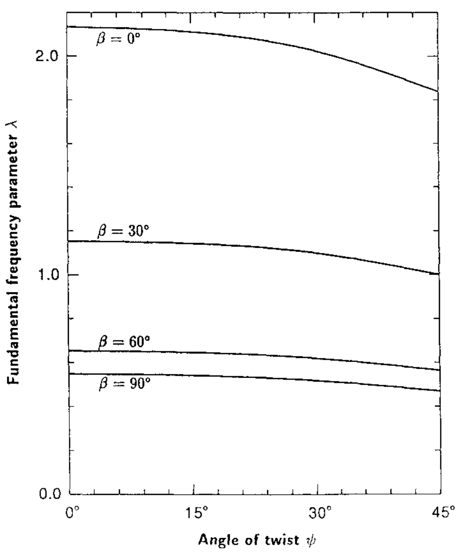

Fig. 5 Effects of angle of twist on the nondimensional fundamental frequency $\lambda = \omega ab\sqrt{(\rho h/D_0)}$ for the 2-ply graphite/epoxy plate with a/b = 2.0, b/h = 100.0, c_r = 0.5, and stacking sequence $(\beta, -\beta)$.

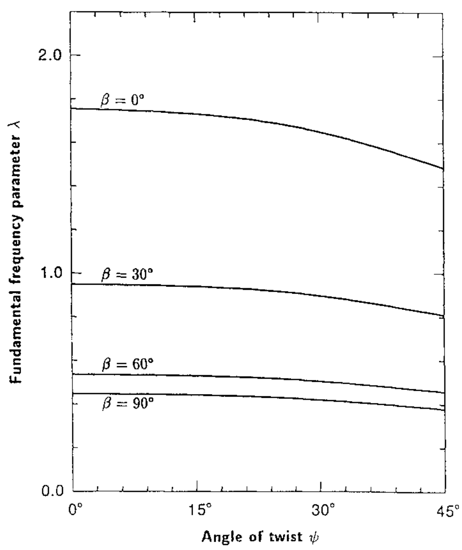

Fig. 6 Effects of angle of twist on the nondimensional fundamental frequency $\lambda = \omega ab\sqrt{(\rho h/D_0)}$ for the 2-ply graphite/epoxy plate with a/b = 2.0, b/h = 100.0, c_r = 1.0, and stacking sequence $(\beta-, \beta)$.

ratio b/h is fixed at 100.0. A set of data covering wide ranges of plate configurations are presented in Tables 3–5 corresponding to 2-ply, 4-ply, and 8-ply laminates. The angle of twist ψ varies from 0 (untwisted) to 45 deg whereas the angle of fiber orientation β changes from 30 to 60 deg.

It is observed in Table 3 that λ for a 2-ply square plate [$a/b = 1.0$ and stacking sequence $(\beta, -\beta)$] decreases when the chord ratio c_r is increased from 0.5 to 1.0. It also generally decreases when β is increased. Similar facts are also noticed for $a/b = 2.0$. In this table, the highest fundamental λ corresponds to $\beta = 30$ deg and $c_r = 0.5$ for a fixed angle of twist. The effects of aspect ratio can be examined in Tables 3–5. Assuming constant ab as explained earlier, increasing a/b renders lower λ and, thus, lower physical frequency ω because a more slender plate has lower structural stiffness.

Table 5 Frequency parameters $\lambda = \omega ab\sqrt{(\rho h/D_o)}$ for the cantilever pretwisted 8-ply graphite/epoxy plate with $a/b = 1.0, b/h = 100.0$, and stacking sequence $(\beta, -\beta, \beta, -\beta, \beta, -\beta, \beta, -\beta)$

a/b	ψ, deg	β, deg	c_r	Mode sequence number 1	2	3	4	5	6	7	8
		30	0.5	3.1328	10.658	16.552	28.798	30.353	45.144	56.519	58.515
	0		1.0	2.6280	6.3513	13.289	16.965	22.539	28.251	37.659	45.438
		60	0.5	1.5057	8.0566	9.4337	22.084	24.923	39.836	43.963	44.485
			1.0	1.2478	5.5468	7.5905	17.877	18.913	23.072	34.055	37.098
		30	0.5	3.1346	16.682	27.680	35.995	43.605	46.327	65.509	65.726
	15		1.0	2.6003	15.811	18.922	21.695	29.078	38.794	45.463	48.978
		60	0.5	1.4949	7.9454	16.965	21.959	36.556	41.696	44.503	55.884
1.0			1.0	1.2354	7.4894	12.924	19.919	23.464	31.585	42.714	44.741
		30	0.5	3.0338	16.060	44.596	50.152	54.688	66.235	81.113	86.089
	30		1.0	2.4854	14.906	30.638	34.164	40.670	45.049	58.806	64.469
		60	0.5	1.4469	7.5894	21.561	30.852	42.676	49.543	59.052	70.992
			1.0	1.1864	7.0894	20.850	24.155	26.580	43.099	49.372	54.584
		30	0.5	2.7672	14.614	43.483	73.401	77.940	87.580	92.782	107.05
	45		1.0	2.2424	13.246	41.409	43.483	48.503	56.069	78.210	86.761
		60	0.5	1.3263	6.9472	20.786	42.105	49.757	59.264	71.755	83.242
			1.0	1.0750	6.3473	20.276	34.469	35.914	42.118	61.466	71.320
		30	0.5	1.5410	8.2441	9.4622	22.591	25.050	39.467	44.825	44.828
	0		1.0	1.2773	5.5651	7.7654	17.975	18.784	23.436	34.372	37.023
		60	0.5	0.72780	3.9257	8.8277	10.733	21.185	22.322	35.331	37.544
			1.0	0.59990	3.7086	5.1704	10.617	15.906	21.147	27.819	33.598
		30	0.5	1.5310	8.1330	17.298	22.473	37.293	41.685	45.116	56.933
	15		1.0	1.2653	7.6688	13.286	20.005	23.722	31.905	43.374	45.331
		60	0.5	0.72015	3.8568	10.662	11.478	21.107	26.956	35.235	44.038
2.0			1.0	0.59307	3.6285	7.8841	10.536	21.086	23.538	33.439	37.390
		30	0.5	1.4824	7.7731	22.075	31.707	43.603	49.604	60.521	72.427
	30		1.0	1.2151	7.2613	21.333	24.943	26.796	44.114	48.838	54.878
		60	0.5	0.69384	3.6511	10.446	17.656	20.878	34.982	38.442	52.645
			1.0	0.56941	3.3959	10.293	13.694	20.899	33.251	37.587	39.524
		30	0.5	1.3586	7.1169	21.287	43.100	51.588	60.062	73.445	85.073
	45		1.0	1.1008	6.4981	20.764	35.322	36.953	43.099	61.692	72.966
		60	0.5	0.63645	3.3129	10.042	20.462	27.289	34.554	52.285	56.706
			1.0	0.51812	3.0341	9.8612	20.521	22.196	33.413	38.287	52.253

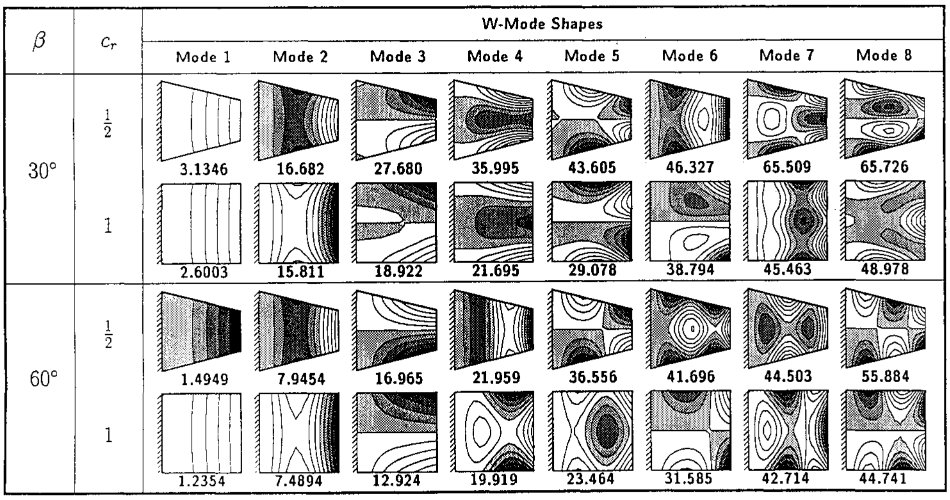

Fig. 7 Effects of angle of lamination and chord ratio on $\lambda = \omega ab\sqrt{(\rho h/D_0)}$ and the transverse vibration mode shapes for the 8-ply graphite/epoxy plate with $a/b = 1.0$, $b/h = 100.0$, $\psi = 15$ deg, and stacking sequence $(\beta, -\beta, \beta, -\beta, \beta, -\beta, \beta, -\beta)$.

The effects of number of plies on λ can be observed by comparing corresponding values in Tables 3–5 for 2-ply, 4-ply, and 8-ply laminates. It is evident that the frequencies are higher for laminates with more plies. For instance, the fundamental λ increases from 2.0113 for $a/b = 1.0$, $\psi = 45$ deg, $\beta = 30$ deg, and $c_r = 0.5$ as shown in Table 3 (2 ply) to 2.6273 in Table 4 (4 ply) and 2.7672 in Table 5 (8 ply). Therefore, the structural stiffness of a pretwisted plate can be increased by having more laminations since the physical frequency ω is directly proportional λ.

The fundamental λ varies as the angle of twist ψ is gradually increased. By observing data in Tables 3–5, the definite ψ corresponding to maximum fundamental λ cannot be determined. This information can be obtained from Figs. 3–6, which correspond to a 2-ply graphite-epoxy plate with $b/h = 100.0$. The aspect ratio

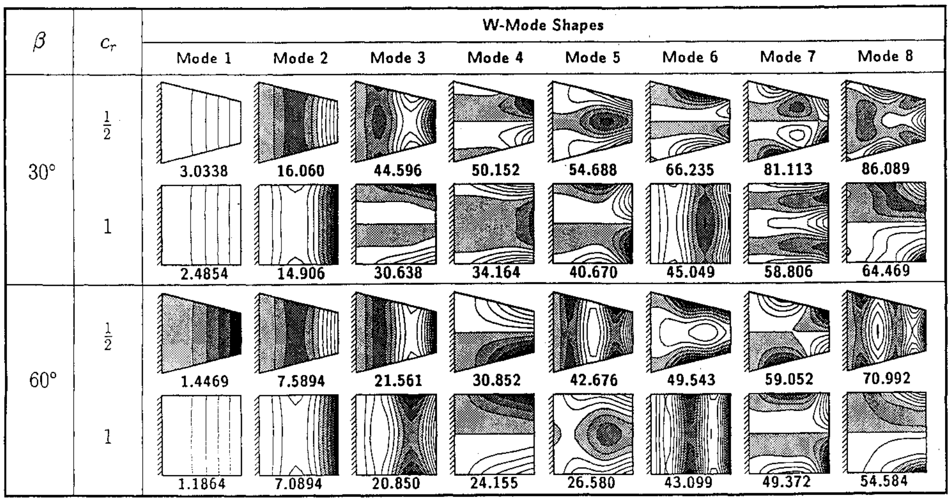

Fig. 8 Effects of angle of lamination and chord ratio on $\lambda = \omega ab\sqrt{(\rho h/D_0)}$ and the transverse vibration mode shapes for the 8-ply graphite/epoxy plate with $a/b = 1.0$, $b/h = 100.0$, $\psi = 30$ deg, and stacking sequence $(\beta, -\beta, \beta, -\beta, \beta, -\beta, \beta, -\beta)$.

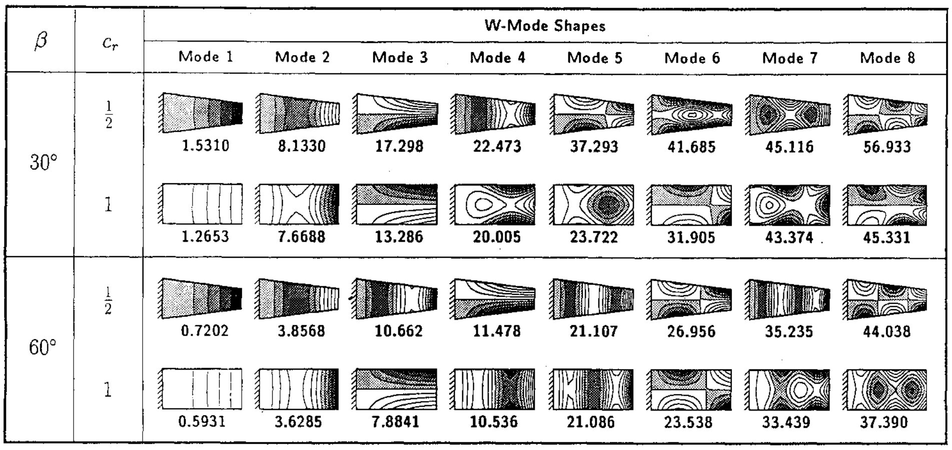

Fig. 9 Effects of angle of lamination and chord ratio on $\lambda = \omega ab\sqrt{(\rho h/D_0)}$ and the transverse vibration mode shapes for the 8-ply graphite/epoxy plate with $a/b = 2.0$, $b/h = 100.0$, $\psi = 15$ deg, and stacking sequence $(\beta, -\beta, \beta, -\beta, \beta, -\beta, \beta, -\beta)$.

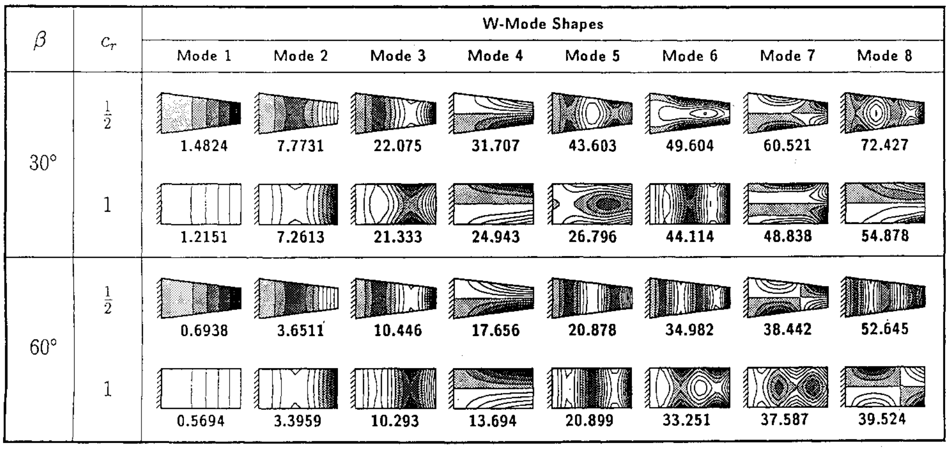

Fig. 10 Effects of angle of lamination and chord ratio on $\lambda = \omega ab\sqrt{(\rho h/D_0)}$ and the transverse vibration mode shapes for the 8-ply graphite/epoxy plate with $a/b = 2.0$, $b/h = 100.0$, $\psi = 30$ deg, and stacking sequence $(\beta, -\beta, \beta, -\beta, \beta, -\beta, \beta, -\beta)$.

a/b changes from 1.0 (Figs. 3 and 4) to 2.0 (Figs. 5 and 6), whereas the chord ratio c_r varies from 0.5 to 1.0. In Fig. 3 ($a/b = 1.0$ and $c_r = 0.5$), the maximum λ occurs in the range of $10 < \psi < 20$ deg for $\beta = 0$ deg and occurs at $\psi = 0$ deg (untwisted plate) for $\beta = 30$, 60, and 90 deg. For $a/b = 1.0$ and $c_r = 1.0$ as shown in Fig. 4, the untwisted plate obviously provides the highest fundamental λ for all values of β. For rectangular plates (Figs. 5 and 6), the maximum fundamental λ again occurs when $\psi = 0$ deg regardless of the chord ratio.

Figures 7–10 illustrate the effects of aspect ratio, chord ratio, angle of twist, and fiber orientation upon the transverse vibration mode shapes for the 8-ply laminates. These plates, however, also have in-plane vibrations in the x and y directions which are not shown here. The shaded contour lines show the regions with negative displacement amplitude and the unshaded contour line otherwise. The lines of demarcation are the nodal lines having zero displacement amplitude. From these figures, it is observed that the first two modes are the spanwise bending modes having 0 and 1 nodal line, respectively, for these cantilever pretwisted laminated plates. The number of nodal lines increases and the vibration modes become more complicated for the higher modes.

V. Conclusions

In this paper, an approximate method based on the extremum energy principle has been developed to study the vibratory characteristics of pretwisted cantilever laminated plate of trapezoidal planform. The Ritz minimization procedure has been employed with a set of orthogonally generated mathematically complete two-dimensional *pb*-2 shape functions as the admissible displacement amplitude functions. The kinematic boundary conditions of the structure are satisfied at the outset because the boundary expressions and constraints have been formulated as the intrinsic components of the *pb*-2 shape functions.

The numerical convergence of this method has been carefully verified through a convergence study. It has been shown that 14 and 18 deg of polynomial for the in-plane (u and v) and transverse (w) deflections were sufficient to provide sound numerical frequencies. The effects of various geometric properties of the graphite/epoxy laminated plate have been thoroughly studied. Increases in the aspect ratio, chord ratio, and angle of lamination decrease the vibration frequencies monotonically; however, the frequency increases for laminates with more plies. In general, the highest fundamental frequencies correspond to untwisted plates except for the case of a square plate with zero degree of lamination and chord ratio 0.5 where the maximum fundamental frequency occurs in between 10 and 20 deg. The effects of plate geometric parameters on the vibration mode shapes have been illustrated in contour mode shapes.

References

[1]Carnegie, W., "Vibrations of Pretwisted Cantilever Blading," *Proceedings of the Institution of Mechanical Engineers*, Vol. 173, No. 12, 1959, pp. 343–374.

[2]Carnegie, W., "Vibrations of Pretwisted Cantilever Blading: An Additional Effect due to Torsion," *Journal of Mechanical Engineering Science*, Vol. 6, No. 2, 1964, pp. 105–109.

[3]Houbolt, J. C., and Brooks, G. W., "Differential Equations of Motion for Combined Flapwise Bending, Chordwise Bending and Torsion of Twisted Nonuniform Rotor Blades," NACA Rept. 1346, 1958.

[4]Montoya, J., "Coupled Bending and Torsional Vibrations in a Twisted Rotating Blade," *Brown Boveri Review*, Vol. 53, No. 3, 1966, pp. 216–230.

[5]Reissner, E., and Washizu, K., "On Torsional Vibrations of a Beam with a Small Amount of Pretwist," *Journal of the Japan Society of Aerospace Engineering*, Vol. 5, No. 47, 1958, pp. 330–335.

[6]Bridle, M. D. J., "Vibration of thick plates and shells," Ph.D. Thesis, Univ. of Nottingham, England, UK, 1973.

[7]Gupta, K., and Rao, J. S., "Torsional Vibration of Pretwisted Cantilever Plates," *Journal of Mechanical Design*, Vol. 100, July, 1978, pp. 528–534.

[8]Leissa, A. W., MacBain, J. C., and Kielb, R. E., "Vibrations of Twisted Cantilevered Plates—Summary of Previous and Current Studies," *Journal of Sound and Vibration*, Vol. 96, No. 2, 1984, pp. 159–173.

[9]Kielb, R. E., Leissa, A. W., and MacBain, J. C., "Vibrations of Twisted Cantilevered Plates—A Comparison of Theoretical Results," *International Journal for Numerical Methods in Engineering*, Vol. 21, No. 8, 1985, pp. 1365–1380.

[10]MacBain, J. C., Kielb, R. E., and Leissa, A. W., "Vibrations of Twisted Cantilevered Plates—Experimental Investigation," *Journal of Engineering for Gas Turbines and Power*, Vol. 107, No. 1, 1985, pp. 187–196.

[11]Chamis, C. C., "Vibration Characteristics of Composite Fan Blades and Comparisons with Measured Data," *Journal of Aircraft*, Vol. 14, No. 7, 1977, pp. 644–647.

[12]Qatu, M. S., and Leissa, A. W., "Vibration Studies for Laminated Composite Twisted Cantilevered Plates," *International Journal of Mechanical Sciences*, Vol. 33, No. 11, 1991, pp. 927–940.

[13]Liew, K. M., and Lim, C. W., "Vibratory Characteristics of Cantilevered Rectangular Shallow Shells of Variable Thickness," *AIAA Journal*, Vol. 32, No. 2, 1994, pp. 387–396.

[14]Liew, K. M., and Lim, C. W., "A Global Continuum Ritz Formulation for Flexural Vibration of Pretwisted Trapezoidal Plates with One Edge Built In," *Computer Methods in Applied Mechanics and Engineering*, Vol. 114, 1994, pp. 233–247.

[15]Leissa, A. W., and Qatu, M. S., "Equations of Elastic Deformation of Laminated Composite Shallow Shells," *Journal of Applied Mechanics*, Vol. 58, March 1991, pp. 181–188.